Research Article

Juntong Zhou, Xiao Wu, Zhanhong Zhao, Zhenpeng Wang, Shumu Li, Chang Chen, Shan Yu, Xintong Qu, Kexin Li, Ye Tian, Xiaojing Liu, Gaoyu Zhang, Zhaoxuan Wang, Chi Li, Ning Kang, Qing Huo*

Preparation of a novel ginkgolide B niosomal composite drug

https://doi.org/10.1515/chem-2020-0089
received April 21, 2020; accepted July 28, 2020

Abstract: Ginkgolide B (GB) and Puerarin (Pue) are active pharmaceutical ingredients for the treatment of Parkinson's disease (PD); however, both are poorly water-soluble, which limits their bioavailability. The present study used the niosome vesicle encapsulation technique to prepare a novel GB composite drug. The conditions for GB–Pue niosomal complex preparation were as follows: a hydration temperature of 60°C, a hydrophilic–lipophilic balance of 10.5, a drug–carrier mass ratio of 8:100, and a surfactant–cholesterol mass ratio of 1.5:1. The niosomal complex suspension was uniformly distributed and milky white in color, with no stratification over a duration of 1 month. It had an average particle size of 187.3 nm, a particle-size distribution of 0.237, a GB encapsulation efficiency (EE) of 68.2%, a GB drug-loading rate of 90.1%, a Pue EE of 40.5%, and a Pue drug-loading rate of 83.3%. The optimal storage temperature for the niosomal complex suspension was 4°C. Following an intravenous injection of the niosomal complex suspension into the rat tail, the area under the curve (AUC) from 0 to 4 h was 54.1 h μg mL^{-1}, with a mean residence time (MRT) of 0.96 h, a distribution half-life ($T_{1/2\alpha}$) of 0.195 h, and a total clearance of 0.003 L h^{-1} kg^{-1}. The AUC and MRT of the composite prescription were 1.1- and 1.4-times those of the commercial injection, respectively, showing significantly increased sustained release and bioavailability. Moreover, the distribution of GB in the brain tissue was 1.8-times that of the commercial injection. In conclusion, the novel GB niosomal composite drug, with excellent stability, improved pharmacokinetics, and brain tissue distribution, demonstrates great potential for the delivery of GB and Pue for PD therapeutics.

Keywords: ginkgolide B, puerarin, niosome, Parkinson's disease

*** Corresponding author: Qing Huo,** Department of Biomedicine, Biochemical Engineering College of Beijing Union University, Beijing-100023, People's Republic of China,
e-mail: huo_q2002@aliyun.com, tel: +86-010-5207-2268,
fax: +86-010-5207-2337

Juntong Zhou, Xiao Wu, Chang Chen, Shan Yu, Xintong Qu, Kexin Li, Ye Tian, Xiaojing Liu, Gaoyu Zhang, Zhaoxuan Wang, Chi Li, Ning Kang: Department of Biomedicine, Biochemical Engineering College of Beijing Union University, Beijing-100023, People's Republic of China

Zhanhong Zhao: School hospital, Beijing Union University, Beijing-100101, People's Republic of China

Zhenpeng Wang, Shumu Li: Analysis and Testing Center, Institute of Chemistry, Chinese Academy of Sciences, Beijing-100190, People's Republic of China

1 Introduction

Alzheimer's disease (AD) is a progressive neurological degenerative disorder, the symptoms of which are not always apparent in the early stages. Currently, the well-recognized pathogenic mechanism of AD is thought to be a persistent abnormal increase in the level of glutamic acid in the brain. Glutamic acid activates G protein coupled receptors, which leads to the overproduction and aggregation of β-amyloid (Aβ), destroying neurons and eventually resulting in neurodegenerative diseases [1–3]. Alberdi et al. reported that ionized glutamic acid may induce abnormal calcium changes, cause Aβ overload, sabotage mitochondrial function, escalate intracellular oxidative stress, promote depolarization of the mitochondrial membrane, and eventually result in neurotoxicity.

Ginkgo biloba belongs to the *Ginkgoaceae* family and contains a variety of effective therapeutic factors such as flavonoid and terpenoid derivatives. Ginkgolide B (GB) accounts for approximately 25% of the total ginkgolides. The efficacy of GB has been demonstrated via the inhibition of platelet-activating factor (PAF). GB is recognized worldwide as an effective substance for the treatment of brain diseases, with only mild adverse effects [4–7]. Intervention with GB has been shown to protect nerve cells damaged by the accumulation of Aβ from

further destruction [8,9]. Using *in vitro* experiments, Xiao et al. showed that GB can diminish the induction of apoptosis by the Aβ (25–35) peptide, suggesting that the mechanism may involve brain-derived neurotrophic factor [10]. Shi et al. indicated that GB has protective and reparative effects on mitochondria damaged by the Aβ (1–42) peptide, in addition to interfering with the activation of amino-terminal kinases and the transmission of abnormal signals in the brain. Currently, GB substances with PAF receptor antagonistic effects are considered capable of effectively interfering with the development of AD and could therefore be used for the treatment of early-stage AD [11,12]. Conventional GB prescriptions include emulsions, powder injections, solid dispersion in the form of dripping pills, and powders. Oral GB liposomes are on the market in Europe to protect the heart and brain blood vessels in the elderly; however, the physicochemical properties of GB, such as high hydrophobicity and high molecular weight, markedly decrease its bioavailability.

Pueraria belongs to the *Leguminosae* family of herbs and its primary active ingredients are flavonoids such as daidzein and puerarin (Pue). The isoflavone of Pue is key to its pharmaceutical applications. Pue has significant positive effects on neurological diseases in the brain, such as AD and Parkinson's disease (PD); however, its therapeutic mechanism is extremely complicated, likely involving three different processes. The first is stabilizing the functions of amino acid neurotransmitters; Pue can maintain the dynamic balance of excitatory and inhibitory amino acids and eliminate nerve cell damage [13–16]. The second is scavenging free radicals; when the body has excessive free radicals, Pue can activate endogenous antioxidants to relieve nervous system damage. The third is interfering with the regulation of neural apoptosis signaling; under detrimental conditions such as ischemia, Pue can activate the PI3-K/Akt pathway and induce gene expression to reduce the degree of damage to neurons and nerve cells [17–19].

GB can affect the metabolism of glutamic acid and dopamine by regulating the D-glutamic acid pathway, thus interfering with the early stage of PD. Intervention of PD with Pue works primarily by increasing endogenous antioxidant activity, regulating calcium signaling pathways, and removing free radicals. The etiology of PD suggests that the structure of L-DOPA in the nigrostriatal area of the brain is affected, increasing the levels of dopamine and free radicals, which destroy the structure of neurons. The two abovementioned drugs can effectively regulate key points in the disease process, protecting and repairing neurons in the brain.

Niosome technology is a novel microparticle preparation method based on liposomes. Non-ionic surfactant niosomes use non-ionic surfactants to ensure that the vesicle excipients are structured as bilayers to encapsulate pharmaceuticals, and the number of structural layers of niosomes can be modified to encapsulate multiple pharmaceutical ingredients [20,21]. The special excipients of non-ionic surfactant vesicles can encapsulate both hydrophilic and lipophilic drugs, enhance their synergism, stabilize their curative effect, improve patient compliance, and avoid the oxidative decomposition issues related to phospholipid molecules [22]. Niosomes are used as an emerging drug delivery system that is in phase III and IV trials in Germany due to the sustained, controlled, and targeted release, convenient administration, good patient compliance, and treatment efficacy for a variety of conditions. During the preparation of niosomes, external forces such as ultrasound and pressure are needed to form the bilayer structure; the hydrophilic–lipophilic balance (HLB) and amphiphilic molecular conformation are key to regulating its formation. Moreover, the inter-bilayer spacing, preparation process, bilayer fluidity, and number of chains in the bilayer structure can also play a role in sustained drug release and targeting. The size of the non-ionic surfactant vesicles is important for allowing passage through various tissues and organs, eliminating the first-pass effect, and penetrating the blood–brain barrier. Modification of membrane materials mainly focuses on the location of the modification and whether it results in the expected targeting effects. Modifications include ferrous ions, strong volatile traditional Chinese herbs, and probes [23,24].

The blood–brain barrier can prevent various pharmaceuticals from reaching the brain, causing difficulties in the treatment of diseases. Using carriers that can facilitate penetration of the blood–brain barrier, such as modified ions, strong volatile Chinese herbs, and probes, helps to reach a drug concentration in its effective range and achieve brain targeting [25–27]. Previous studies have investigated strong volatile Chinese herbs and found that mint and gabardine can relax the endothelial cells constituting the blood–brain barrier, which temporarily enhances the permeability of pharmaceuticals.

There exist various pathogenic theories for PD. In the present study, three theories, oxidative stress, neurotoxicity, and dopamine abnormality, were used as references to select drugs and the site of action. By controlling the dynamic balance of dopamine, free radicals, and glutamic acid in multiple brain areas, the remission and treatment of PD could be achieved. While most of the available marketed drugs are a single-drug therapy, we attempted to target two sites for the treatment and control of PD by studying a composite drug of GB and Pue. GB could reduce the abnormal level of dopamine since it stimulates the conversion of

L-DOPA to dopamine, and Pue could decrease the excessive level of free radicals since it acts as a scavenger. One of the primary reasons why many pharmacological treatments for PD fail to achieve the desired effect is their inability to cross the blood–brain barrier, which has a certain blocking effect on drug molecules above the nanoscale. Studies on traditional Chinese medicine have demonstrated that certain aromatic drugs have a temporary weakening effect on the blood–brain barrier, effectively allowing the drug to cross in the brain. In the present study, borneol was applied onto the niosomal bilayer to facilitate the uptake of the vesicles into the brain, allowing GB and Pue to exert their pharmacological effects.

In the present study, poorly water-soluble GB and Pue were used to prepare a novel brain-targeted drug. Glyceryl monostearate (GMS), MYRJ49, and cholesterol were employed as excipients to prepare niosomes encapsulating GB and Pue, and the niosome surfaces were modified with volatile borneol.

2 Materials and methods

2.1 Experimental materials

GB (93% content), GB standard, Pue (90% content), and Pue standard were purchased from Sichuan Pharmaceutical Co., Ltd (Sichuan, China). GMS was purchased from Guangzhou Kafen Biotech Co., Ltd. MYRJ 49 was purchased from Guangzhou Donglin Fine Chemical Co., Ltd. Cholesterol, glucose, sodium chloride, dimethyl sulfoxide (DMSO), and Tween® 80 were purchased from Beijing Mengyimei Bio-Tech Co., Ltd. Borneol was purchased from Shanghai Puda Chemical Co., Ltd. A total of 20 male Wistar rats, weighing 200 ± 20 g and fed a standard diet, were used. All animals and feed were obtained from the Beijing University of Traditional Chinese Medicine.

2.2 Experimental instrumentation

The following instrumentation was used: high-performance liquid chromatography (HPLC) 1200 system (Agilent Technologies); rotary evaporator RE-2000 (Shanghai Yarong Biochemical Instrument Factory); low-temperature cooling liquid circulating pump (Zhengzhou Greatwall Scientific Industrial and Trade Co., Ltd); high-pressure homogenizer (Shanghai Shenlu Homogenizer Co., Ltd); ultrasonic cell pulverizer (Ningbo Scientz Biotechnology Co., Ltd); zetasizer (Malvern Instruments, UK); comprehensive drug stability test chamber (Hangzhou Junsheng Scientific Equipment Co., Ltd); CO_2 cell culture incubator (Suzhou Proxy Water Experiment Equipment Co., Ltd); inverted phase contrast microscope (Shanghai Yuyan Instruments Co., Ltd); ultra-high-performance liquid chromatograph mass spectrometer (UHPLC-MS) Shimadzu LCMS-8050 (Shanghai Yidian Analytical Instrument Co., Ltd).

2.3 Experimental methods

2.3.1 HPLC analysis of GB

The GB standard solutions were prepared and subjected to ultraviolet (UV) detection according to the Pharmacopoeia of the People's Republic of China 2015 Edition. The HPLC settings were as follows: mobile phase of methanol:0.2% aqueous phosphoric acid solution = 33:67; flow rate of 1 mL/min; wavelength of 205 nm; column temperature of 30°C; and injection volume of 20 µL. The y-axis represented the GB peak area and the x-axis represented the GB standard concentration, resulting in a linear equation of $y = 521.2x + 13.675$, $R^2 = 0.9990$, with a regression interval of 0.1–1.5 mg/mL (Figure 1).

2.3.2 HPLC analysis of Pue

The Pue standard solutions were prepared and subjected to UV detection according to the Pharmacopoeia of the People's Republic of China 2015 Edition. The HPLC settings were as follows: mobile phase of methanol:0.5% aqueous phosphoric acid solution = 30:70; flow rate of 1 mL/min; wavelength of 264 nm; column temperature of 30°C; and injection volume of 20 µL. The y-axis represented the Pue peak area and the x-axis represented the Pue standard concentration, resulting in a linear equation of $y = 53{,}511x - 2303.7$, $R^2 = 0.9992$, with a regression interval of 0.1–1.5 mg/mL (Figure 2).

2.3.3 Preparation of the niosomal complex suspension

(1) Appropriate amounts of GMS, MYRJ 49, and cholesterol were dissolved in a homogeneous mixture of

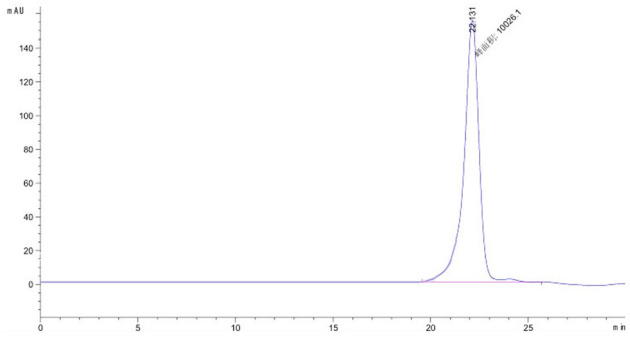

Figure 1: GB standard solution

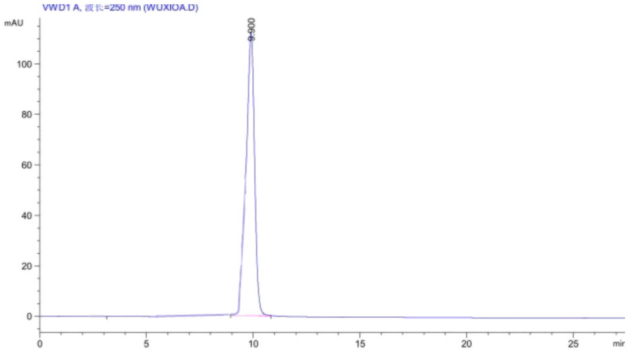

Figure 2: Pue standard solution

DMSO:methanol (1:3) and subjected to reduced pressure at 55°C until all solvents had volatilized to leave a thin film.

(2) The prepared thin film was dissolved in an appropriate amount of organic reagent, added to alcohol and buffer containing an appropriate amount of drug (GB–Pue mass ratio of 1:1), and shaken for 20 min. Subsequently, an appropriate amount of buffer was added and hydration was carried out for 15 min, followed by the addition of borneol at room temperature.

(3) The niosomal complex suspension was further homogenized using a high-pressure homogenizer (1,000 bar, four times).

Note: Phosphate-buffered saline (PBS) (pH = 6.8); a precise volume of 250 mL of 0.2 mol/L potassium dihydrogen phosphate solution and 118 mL of 0.2 mol/L aqueous sodium hydroxide solution were transferred to a 1 L volumetric flask and distilled water was added to a final volume of 1 L; borneol was pulverized using a mortar and pestle; the surface active agent in Table 1 was Reviewer #1-(a mixture of GMS and MYRJ 49; the carrier was surfactant (GMS and MYRJ 49) and cholesterol.

Scoring criteria:

(1) The scoring of encapsulation efficiency (EE): 80% = 40 points.

(2) The scoring of drug loading: 60% = 30 points.

(3) The scoring of particle size: (0.05–0.10] μm = 20 points; (0.10–0.15] μm = 16 points; (0.15–0.20] μm = 12 points; (0.20–0.25] μm = 8 points; (0.25–0.30] μm = 4 points; (0.30–0.50] μm = 2 points; and >0.50 μm = 0 points.

(4) The scoring of PDI: (0.05–0.10] = 10 points; (0.10–0.15] = 8 points; (0.15–0.20] = 6 points; (0.20–0.30] = 4 points; (0.30–0.50] = 2 points; (0.50–1.00] = 1 point; and >1 = 0 points.

2.3.4 Evaluation of the niosome quality

2.3.4.1 EE of niosomes

(1) The niosomal suspension was transferred to a centrifuge tube using a pipette and centrifuged at 4,000 rpm for 20 min. The upper layer was collected and diluted to obtain W_f.

(2) An appropriate amount of the lower layer was transferred to a centrifuge tube using a pipette, demulsified with methanol, shaken thoroughly, diluted, and filtered through a microporous membrane to obtain W_i.

$$\text{EE } (\%) = W_i/(W_f + W_i) \times 100$$

Table 1: Factors and levels of orthogonal experimental design

Levels	Factors			
	(A) Temperature (°C)	(B) Surfactant–cholesterol ratio	(C) Drug–carrier ratio	(D) HLB
1	50	1.25:1	8:100	10.0
2	55	1.50:1	9:100	10.5
3	60	1.75:1	10:100	11.0

2.3.4.2 Drug loading

(1) The niosomal suspension was transferred to a centrifuge tube using a pipette, to which an appropriate amount of methanol was added. The solution was transferred to a homogenizer to break the vesicles.
(2) The above solution was filtered through a microporous membrane to measure the total drug concentration W_t.

2.3.4.3 Storage condition testing

GB, Pue, and the GB–Pue niosomal complex suspension were placed at 4°C and 25°C and stored in sealed glass bottles for 0, 7, 14, 21, 28, 35, and 60 days.

2.3.5 *In vivo* pharmacokinetics and brain distribution of the niosomal complex suspension in rats

In the present study, the route of administration was intravenous bolus injection in the rat tail. The concentration was 12.7 μg/mL GB for prescription 1 and 12.9 μg/mL GB for prescription 2. The administered volume was 4 mL (administered according to the dose) and the injection dose was 200 μg/kg.

Each experimental group contained six male Wistar rats that were fasted overnight for 12 h, weighed, and administered drugs according to weight. Approximately 0.8 mL of blood was sampled from the rat eye socket vein prior to administration and 5, 15, 30 min, and 1, 2, 3, and 4 h following administration. The blood sample was transferred to a heparin anticoagulant tube, centrifuged to prepare plasma, acidified with hydrochloric acid (100 μL of 1 mol/L hydrochloric acid per 1.0 mL plasma), and stored in a −20°C freezer. The present study was performed according to the international rules considering the animal experiments and biodiversity rights (Ethical Approval Council Number: 2020-02).

A volume of 10 μL fluconazole internal standard (10 μg/mL) was added to 0.2 mL acidified plasma sample and vortexed for 30 s, to which 1 mL of ethyl acetate was added, and the solution was shaken for 2 min and subsequently centrifuged at 6,000 rpm for 5 min. An 800 μL aliquot of the supernatant was dried under nitrogen at 40°C in a water bath. The 100 μL residual was dissolved in acetonitrile, vortexed for 30 s, and centrifuged, and the resulting supernatant was transferred to a HPLC vial.

2.3.6 Preparation of brain tissue samples

Prescription 1 contained 12.7 μg/mL GB and prescription 2 contained 12.9 μg/mL GB in an administered volume of 4 mL (same as above). The rats were euthanized by cervical dislocation 2 h after administration. The brain tissue was then extracted, rinsed with cold saline to remove the superficial blood and debris, wiped clean with dry tissues, and weighed. Subsequently, methanol was added to the brain samples at an overall sample–methanol ratio of 1:3, which were then subjected to homogenization for 15 clockwise and 15 counterclockwise rotations at a constant speed until a uniform milky white-colored homogenate formed. Volumes of 200 μL methanol and 10 μL fluconazole internal standard (10 g/mL) were added to 800 μL brain homogenate, vortexed for 1 min, and centrifuged at 12,000 rpm for 3 min. An 800 μL aliquot of the upper layer was dried under nitrogen. The 100 μL residuals were dissolved in acetonitrile, vortexed for 30 s, and centrifuged, and the resulting supernatant was transferred to a HPLC vial.

Note: Prescription 1: 0.025 mg GB, 0.2009 mg GMS, 0.2991 mg MYRJ 49, and 0.375 mg cholesterol. Prescription 2: 0.025 mg GB, 0.025 mg Pue, 0.2009 mg GMS, 0.2991 mg MYRJ 49, 0.375 mg cholesterol, and 5 mg borneol.

2.3.7 LC-MS analysis

The LC-MS analysis was conducted using a UHPLC-MS Shimadzu LCMS-8050 system consisting of a Shimadzu LC-30AD (including an LC 30A binary pump, an SIL-30AC autosampler, an SPD-M30A photodiode array detector, and a CTO-20AC column oven) and an 8050 triple quadrupole MS.

For liquid phase separation, a Phenomenex Kinetex® C18 column (100 mm × 2.1 mm i.d.: 2.6 μm) was used. The mobile phase was acetonitrile (A) and 0.2% formic acid in water (B), with a flow rate of 0.5 mL min^{-1}, isocratic, and A:B of 35:65. The column temperature was set to 30°C, and the injection volume was 1 μL.

The MS parameters were as follows: a drying gas flow rate of 10 L min^{-1}; a nebulization gas flow rate of 3 L min^{-1}; a heating gas flow rate of 10 L min^{-1}; an interface voltage of 3 kV; a detector voltage of 1.8 kV; an interface heater temperature of 300°C; a desolvation line temperature of 250°C; a block heater temperature of 400°C; ionization mode ESI negative; and MS mode multiple reaction monitoring.

A precise volume of 0.2 mL blank plasma was added to sequentially diluted GB standards to yield GB concentrations of 0.1, 0.5, 1, 5, 10, 100, and 500 μg/mL (seven samples). After processing as described in the plasma preparation method for HPLC, the samples were subjected to LC-MS with the settings as given in 2.3.6.5 at a wavelength of 207 nm. The y-axis represented the standard GB–fluconazole ratio and the x-axis represented the plasma GB concentration, resulting in a linear regression equation of $y = 0.0159x + 0.006$, $R^2 = 0.9999$.

2.3.8 Statistical analysis of pharmacokinetics

Data were analyzed using DAS 2.0. WinNonlin was used to determine the area under the curve (AUC) from 0 to 240 min, biological half-life ($T_{1/2}$), apparent volume of distribution (V_c), total clearance (CL), elimination rate constant from the central compartment (K_{10}), distribution rate constant of the drug from the central to the peripheral compartments (K_{12}), and distribution rate constant of the drug from the peripheral to the central compartments (K_{21}).

3 Results and analysis

3.1 Effects of organic solvents on niosomal preparation

For the preparation of the niosomal complex suspension, GMS, MYRJ 49, and cholesterol were used as the vesicle excipients. In comparison with Tween® 80 and Span® 80 used in previous vesicle preparation studies, the excipients selected in the present study do not harm the human body over a wide range of concentrations, since GMS and MYRJ49 are food-grade materials primarily used in the manufacture of ice cream and cream, and are safe and non-toxic with no adverse effects.

As shown in Table 2, the two types of non-ionic surfactants, GMS and MYRJ 49, were both soluble in the listed organic solvents. Cholesterol dissolved well in diethyl ether, dichloromethane, and the dichloromethane–methanol mixed solvents. GB and Pue were soluble in methanol, ethanol, and diethyl ether, but did not dissolve well in dichloromethane. Considering both the excipients and drugs, the dichloromethane–methanol (1:3) mixture was selected as the experimental solvent.

3.2 Optimization of the niosomal complex suspension prescription

The hydration temperature, HLB, and non-ionic surfactant are important factors that affect the preparation of niosomes, which in turn determine the therapeutic effect of the encapsulated drugs. In addition, different prescriptions have an impact on the functional characteristics, such as hydrophilicity, lipophilicity, sustained release, and targeting.

On the basis of univariate analysis, orthogonal experiment design is shown in Table 1 to optimize the formulation and the results were obtained, as presented in Table 3. Orthogonal analysis of variance (ANOVA) was obtained, as presented in Table 4.

As shown in the ANOVA table of the niosomal complex suspension, the four factors, hydration temperature, surfactant–cholesterol mass ratio, drug–carrier mass ratio, and HLB, had significant effects on the mean particle size, particle-size distribution, EE, and drug loading, in the order of A > B > D > C. The optimal combination was $A_3B_2C_1D_2$, that is, a hydration

Table 2: Screening of organic solvents

Organic reagent	Dissolving state				
	GMS	MYRJ 49	cholesterol	GB	Pue
Methanol	–	–	–	+	+
Ethanol	–	–	–	+	+
Diethyl ether	+	+	+	+	+
Acetone	+	+	–	+	–
Dichloromethane	+	+	+	–	–
Dichloromethane–methanol (1:1)	+	+	+	–	–
Dichloromethane–methanol (1:2)	+	+	+	–	–
Dichloromethane–methanol (1:3)	+	+	+	+	+

Note: "–" represents incompletely dissolved and "+" represents completely dissolved.

temperature of 60°C, a surfactant–cholesterol mass ratio of 1.5:1, a HLB of 10.5, and a drug–carrier ratio of 8:100.

The hydration temperature used during the preparation process controls the arrangement of side branches in the niosomal bilayer. As the hydration temperature approaches the phase transition temperature of the membrane, the cross-sectional area of the bilayer becomes larger, the chromatographic intervals of the bilayer molecules are reduced, and the fluidity of the membrane is increased. The niosomes formed in this state have a superior drug loading, EE, and particle size. The non-ionic surfactant used in the present study contained no electrons, making the niosomes neutral and reducing the effect of external charges. However, a niosomal membrane composed of only surfactant would result in poor fluidity and instability. The addition of a certain amount of cholesterol would result in encapsulation in the bilayer to regulate membrane fluidity. Different compositions of non-ionic surfactants will produce pharmaceutical preparations with different HLB values. In the present study, the HPB of the pharmaceutical preparations was maintained in both the hydrophilic and lipophilic ranges, conducive to different clinical applications and expanding the scope of drug application. During niosomal complex suspension preparation, ultrasound and homogenization steps were included; the former dispersed the adhered vesicles and the pressure of the latter ensured a nanoscale vesicle particle size, providing an optimal particle dispersion.

All three batches of the prepared niosomal solution were milky white in color and showed no stratification (Figure 3). A small amount of niosomal suspension was placed on a slide, covered with a coverslip, and subjected to optical microscopy at a magnification of 1,000×. The morphologies are shown in Figures 4 and 5.

3.3 Storage conditions

As shown in Figure 6, the EE and physicochemical properties of the niosomal complex suspension were better preserved following storage at 4°C than at 25°C and demonstrated good stability. A low-temperature environment maintained the ordered arrangement and good fluidity of molecules in the bilayer, allowing the membrane to retain a stable framework and providing the niosomes with a higher stability.

3.4 *In vivo* pharmacokinetics and brain distribution of the niosomal complex suspension in rats

3.4.1 Pharmacokinetics

The niosomal complex suspension and commercial GB injections were intravenously administered to rats and the pharmacokinetic parameters of GB were determined.

Table 3: Orthogonal table of the niosomal complex suspension prescriptions

No.	Factor				Particle size (nm)	Particle size distribution	Total drug loading (%)	Total EE (%)	Overall score
	A	B	C	D					
1	50	1.25:1	8:100	10	159.45	0.321	81.92	60.63	50.22
2	50	1.5:1	9:100	10.5	142.65	0.261	82.76	49.90	54.53
3	50	1.75:1	10:100	11	199.8	0.326	72.55	49.85	47.99
4	55	1.25:1	9:100	11	345.9	0.322	64.65	35.45	44.97
5	55	1.5:1	10:100	10	250.1	0.349	68.05	38.95	38.53
6	55	1.75:1	8:100	10.5	174.35	0.313	84.13	50.45	47.74
7	60	1.25:1	10:100	10.5	155.25	0.314	78.78	46.84	50.33
8	60	1.5:1	8:100	11	246.6	0.165	80.37	49.80	52.86
9	60	1.75:1	9:100	10	283.85	0.341	62.91	37.52	43.26
*K*1	54.75	53.92	57.11	51.1					
*K*2	45.65	56.69	49.59	57.65					
*K*3	57.97	47.77	51.68	49.64					
K	12.32	8.92	7.52	8.01					
Factors	A > B > D > C								
Optimal combination	$A_3B_2C_1D_2$								

Note: A is the hydration temperature; B is the surfactant–cholesterol mass ratio; C is drug–carrier ratio; and D is the HLB. The total EE and total drug loading were determined by the EE and drug loading of the two drugs together, $R = R1/2 + R2/2$.

Table 4: Orthogonal ANOVA of the EE of GB in the niosomal complex suspension

	Type III sum of squares	Df	Mean square	*F*	Sig.
Temperature	1603.008	2	801.504	737.580	0.000
Surfactant–cholesterol ratio	48.401	2	24.201	22.270	0.000
Drug–carrier ratio	2031.034	2	1015.517	934.525	0.000
HLB	397.981	2	198.991	183.120	0.000

Figure 3: Niosomal complex suspension.

Figure 4: Microscopic morphology of blank niosomes (1,000×).

The pharmacokinetics of GB in rats were fit to a two-compartment model, as shown in Table 5 and Figures 7–9. Prescription 1 was a GB and Pue niosomal composite drug free of borneol; prescription 2 was a GB-, Pue-, and borneol-containing niosomal composite drug; and INJ was a commercial injection.

Figure 5: Microscopic morphology of niosomal complex suspension vesicles (1,000×).

Table 5 and Figures 7–9 display the mean GB concentration in plasma and variations in the pharmacokinetic parameters of GB within 4 h of intravenous injection. Prescriptions 1 and 2 exhibited no clear differences in the pharmacokinetic profile. Both niosomal complexes suspension demonstrated a significantly higher total GB concentration in plasma as compared with the commercial injection, and the AUC value for prescription 1 was 1.1-times that of the commercial injection, indicating that application of the niosome technique may significantly increase the bioavailability of drugs. The distribution half-life ($T_{1/2\alpha}$) and elimination half-life ($T_{1/2\beta}$) of GB were also significantly enhanced as compared

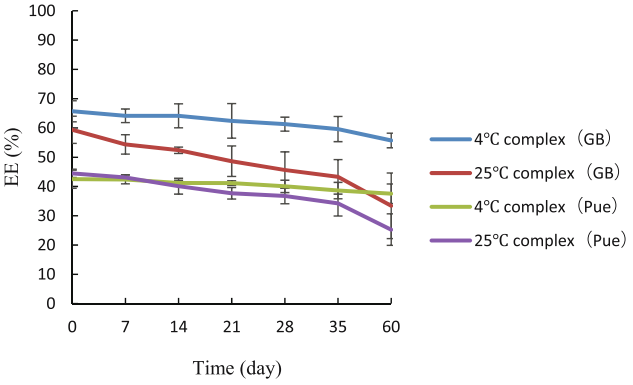

Figure 6: EE stability of GB and Pue in the niosomal complex suspension.

with those of the commercial injection, indicating that niosomes may be able to slowly release the drug *in vivo*. The decrease in CL indicates that the drug clearance was slowed and the residence time was increased.

Comparing prescription 1 with prescription 2, the $T_{1/2\alpha}$ values indicate that prescription 1 absorbed slower, the MAT and $T_{1/2\beta}$ values indicate that prescription 1 stayed longer in the body, and the K_{21} values indicate that prescription 1 was distributed more slowly from the tissue to the blood, suggesting that the drug stayed longer in tissues and organs and was better targeted.

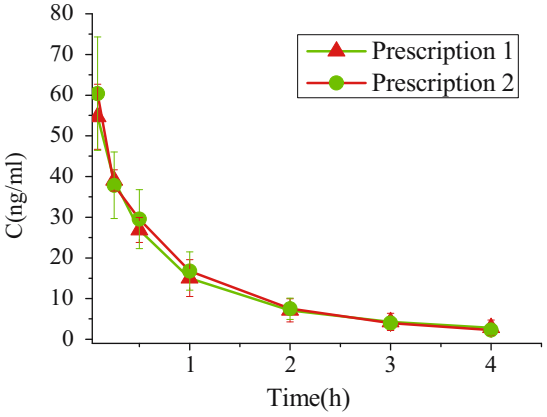

Figure 7: Comparison of sustained release between the two prescriptions.

3.4.2 Distribution in the brain

Brain tissue was extracted and homogenized 2 h following the intravenous injection of GB niosomes in the rat tail, and the GB concentration in brain tissue was determined (Figure 10).

The GB concentration in the rat brain following the borneol-containing niosomal complex suspension, borneol-free niosomal complex suspension, and commercial injections was significantly different 2 h following the intravenous injection, indicating that the drug encapsulated by niosomes could effectively traverse the blood–brain barrier and reach brain cells. There was no significant difference in brain GB level between the borneol-containing and borneol-free complexes. The modification effects and addition methods of borneol require further investigation.

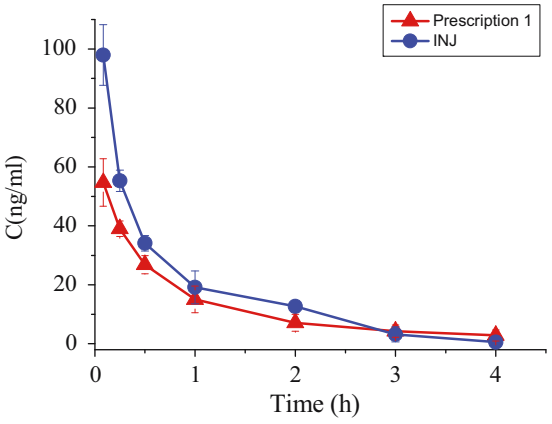

Figure 8: Comparison of sustained release between prescription 1 and the commercial injection.

4 Conclusion

The optimal prescription of the GB–Pue niosomal composite drug was a hydration temperature of 60°C, a surfactant–cholesterol mass ratio of 1.5:1, a HLB of 10.5, and a drug–carrier mass ratio of 8:100. Pharmacokinetics and brain tissue distribution studies demonstrated that niosome technology, by encapsulating the drug in a bilayer, enables

Table 5: Fitting to a two-compartment model

Pharmacokinetic parameters	Prescription 1	Prescription 2	INJ
AUC_{0-4h} (h μg mL^{-1})	54.082 ± 8.201	56.666 ± 12.802	48.800 ± 6.80
Mean residence time (h)	0.955 ± 0.164	0.665 ± 0.43	0.706 ± 0.23
$T_{1/2\alpha}$ (h)	0.195 ± 0.155	0.952 ± 0.107	0.075 ± 0.05
$T_{1/2\beta}$ (h)	2.153 ± 1.199	0.883 ± 0.228*	0.480 ± 0.21
K_{10} (h^{-1})	15.313 ± 23.185	13.758 ± 21.569	4.542 ± 2.41
K_{12} (h^{-1})	10.101 ± 17.438	9.484 ± 16.058	4.818 ± 3.59
K_{21} (h^{-1})	1.061 ± 0.807	2.259 ± 0.863*	1.348 ± 1.09
V_c (L/kg)	0.002 ± 0.001	0.002 ± 0.002	0.997 ± 0.48
CL (L h^{-1} kg^{-1})	0.003 ± 0.001	0.003 ± 0.001	2.890 ± 1.63

Note: Each value represents the mean ± SD (n = 3). *p < 0.05 as compared with INJ.

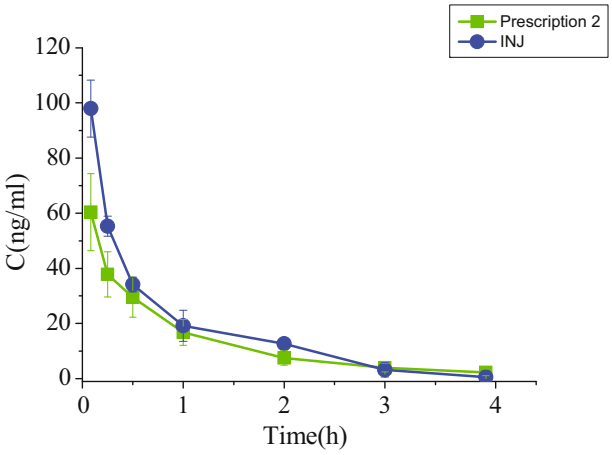

Figure 9: Comparison of sustained release between prescription 2 and the commercial INJ.

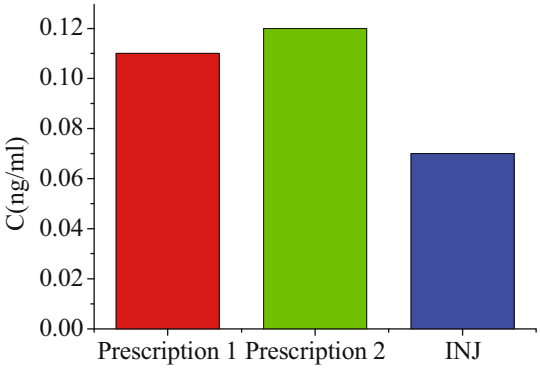

Figure 10: GB concentration in brain tissue.

sustained release and penetration of the blood–brain barrier, extending its half-life and altering the drug distribution in human tissues and organs.

In the present study, pharmacokinetics and brain tissue distribution experiments showed that the prepared niosomal complex suspension had significant sustained release and improved blood–brain barrier penetration. The niosome technology and application of borneol enhanced the sustained release of the drug and its ability to traverse the blood–brain barrier, providing a foundation for the treatment of brain diseases, such as Parkinson's and AD, with GB and Pue composite drugs. Nevertheless, the location of borneol modification and the enhancement of blood–brain barrier penetration require further exploration.

Acknowledgments: This research work was financially supported by the National Natural Science Foundation of China (Grant No. 11975048) and the Beijing Union University Graduate Program.

Conflict of interest: Authors declare no conflict of interest.

References

[1] Dan L, Jiahe W. Research progress of ginkgo biloba extract in preventing and treating Alzheimer's disease. Pract Geriatr. 2017;31(7):609–12.

[2] Shanying P, Wenhui L, Zhengui N, Yang L, Lin W, Feng W, et al. Effects of ginkgolide B on NO, IL-6 and RANTES released by astrocytes. Acta Pharm Sin. 2010;45(9):1103–8. doi: 10.16438/j.0513-4870.2010.09.002.

[3] Bing B, Hailan S, Kehan S. Research status of active components in ginkgo biloba. Sci Technol Innov Herald. 2008;2:96. doi: 10.16660/j.cnki.1674-098x.2008.02.081.

[4] Jinsheng G, Yousong L. Research progress on pharmacological effects of ginkgolide B, Heilongjiang J Tradition Chinese Med. 2011;40(6):62–3.

[5] Ruixia G, Zhi L, Ligeng L, Changhong H, Qingwen S. History of natural medicinal chemistry: Ginkgolides. Chinese Tradition Herb Drugs. 2013;44(6):641–5.

[6] Dingqiang L, Jun C. Pharmacological effects of ginkgolides. J Jiangsu Univ (Nat Sci Ed). 2001;22(2):5–9.

[7] Ting G, Wenwen S, Jiajia W, Wenzhe H, Zhenzhong W, Wei X. Research progress of lactones in ginkgo biloba leaves. China J Chinese Mater Med. 2018;43(7):1384–91. doi: 10.19540/j.cnki.cjcmm.20180312.001.

[8] Hongying G. Effect of ginkgolide injection adjuvant treatment on neurological function recovery in hypertensive cerebral hemorrhage perioperative period. J Hainan Med Univ. 2018;24(12):1203–6+11. doi: 10.13210/j.cnki.jhmu.20180424.006.

[9] Xinhong T, Li H, Yanwen Y, Yuying X, Shiqi Y. Effects of ginkgolide B on expression of Synapsin-1, Beclin1 and LC3 in hippocampus of rats with Alzheimer's disease. Chinese J Basic Med Tradition Chinese Med. 2017;23(12):1701–4+59.

[10] Ibrahima D, Amir F, Ashley IB, Scott A. Cerebrospinal fluid ferritin levels predict brain hypometabolism in people with underlying β-amyloid pathology. Neurobiol Dis. 2019;124(10):335–9. doi: 10.1016/j.nbd.2018.12.010.

[11] Fatima ZS, Mostafa EI, Oana C, Adriana T, Monica H, Lucian H, et al. Tetraclinis articulata essential oil mitigates cognitive deficits and brain oxidative stress in an Alzheimer's disease amyloidosis model. Phytomed. 2019;56(32):57–65. doi: 10.1016/j.phymed.2018.10.032.

[12] Syed OR, Bibhu PP, Suhel P, Madhu K, Salman H, Mohd A, et al. Neuroprotective role of astaxanthin in hippocampal insulin resistance induced by Aβ peptides in animal model of Alzheimer's disease. Biomed Pharmacother. 2019;110(43):47–58. doi: 10.1016/j.phymed.2018.10.032.

[13] Yu Z, Xue Y, Xu HG, Fa YZ. Puerarin attenuates neurological deficits via Bcl-2/Bax/cleaved caspase-3 and Sirt3/SOD2 apoptotic pathways in subarachnoid hemorrhage mice. Biomed Pharmacother. 2019;109(1):726–33. doi: 10.1016/j.biopha.2018.10.161.

[14] Liu SY, Qu XH, Jin GH, Nie F, Liu F, Chen SM, et al. Puerarin promoted proliferation and differentiation of dopamine-producing cells in Parkinson's animal models. Biomed

Pharmacother. 2018;106(20):8854–64. doi: 10.1016/j.biopha.2018.07.058.
[15] Biang J, Liu JH, BaoY M, An LJ. Hydrogen peroxide-induced apoptosis in pc12 cells and the protective effect of puerarin. Cell Biol Int. 2003;27(12):1025–31. doi: 10.1016/j.cellbi.2003.09.007.
[16] Gang W, Li Z, Ying BZ, Miao XD, Xiao ML, Ji CL, et al. Implication of the c-Jun-NH 2 -terminal kinase pathway in the neuroprotective effect of puerarin against 1-methyl-4-phenylpyridinium (MPP +)-induced apoptosis in PC-12 cells. Neurosci Lett. 2010;487(1):88–93. doi: 10.1016/j.neulet.2010.10.002.
[17] Xiongfeng H, Jianmin W. Research progress on neuroprotective mechanism of puerarin. Chinese J Exp Tradition Med Formulae. 2015;21(4):224–30. doi: 10.13422/j.cnki.syfjx.2015040224.
[18] Rong L, Lingyuan X, Tao L, Shijun Z, Yongwen L, Xiaoqun D. Protective effects of puerarin on neurons in substantia nigra of Parkinson's disease model rats induced by 6-hydroxydopamine. Chinese J Exp Tradition Med Formulae. 2013;19(2):247–50. doi: 10.13422/j.cnki.syfjx.2013.02.076.
[19] Rong L, Lingyuan X, Tao L, Xioaqun D, Yongwen L, et al. Effect of puerarin on HO-1 and NQO1 expression in substantia nigra of Parkinson's disease rats. Chinese J Exp Tradition Med Formulae. 2013;19(5):237–40. doi: 10.13422/j.cnki.syfjx.2013.05.083.
[20] Hanan M, Alhar B, Robert B, Campbell V. Nano-formulations composed of cell membrane-specific cellular lipid extracts derived from target cells: physicochemical characterization and in vitro evaluation using cellular models of breast carcinoma. AAPS Open. 2018;4(1):1–9. doi: 10.1186/s41120-018-0025-1.
[21] Samuel I, Mattern S, Richard KF, Philip C, Lauren B, Grimsley TM, et al. CellMimetic liposomal nanocarriers for tailored delivery of vascular therapeutics. Chem Phys Lipids. 2018;218(9):149–57. doi: 10.1016/j.chemphyslip.2018.12.009.
[22] Michaela B, Gerhard W. Vesicular phospholipid gels as drug delivery systems for small molecular weight drugs, peptides and proteins: state of the art review. Int Pharm. 2018;557(30):1–8. doi: 10.1016/j.ijpharm.2018.12.030.
[23] Yongpeng Y, Ping D, Xialin Z, Yu D, Xiaoliang Z, Hong L, et al. Part IV: application prospect of transdermal drug delivery carriers in future cosmetics. China Cosmet Rev. 2010;12:72–6.
[24] Xiaoyan Z, Qineng P. Preparation and *in vitro* evaluation of docetaxel albumin nanoparticles. Progr Pharm Sci. 2008;32(5):223–8.
[25] Liping W, Jianfang F, Kaili H. Research progress on regulatory effect and mechanism of Aroma-inducing traditional Chinese medicine on blood-brain barrier permeability. China J Chinese Mater Med. 2014;39(6):949–54.
[26] Juan J, An Z, Yazhong Z, Li Z. Research progress of Aroma-inducing Chinese medicine in promoting drug absorption *in vivo*. J Jiangxi Univ Tradition Chinese Med. 2016;28(2):106–9.
[27] Caixia Y, Qiuju Z, Mingshua X, Weiping Z, Xue Y, Shunan L, et al. Research progress on effect of borneol on permeability of blood-brain barrier and its promoting effect on drugs. J Gansu Univ Chinese Med. 2018;35(4):96–9. doi: 10.16841/j.issn1003-8450.2018.04.23.